CERN LIBRARIES, GENEVA

CM-P00062313

CERN - EUROPEAN ORGANIZATION FOR NUCLEAR RESEARCH

CERN/EP 79-61

27 June 1979

DIMUON RESONANCE PRODUCTION FROM 200 AND 280 GeV/c TAGGED HADRON BEAM

C.E.N.,Saclay[1]-CERN[2]-Collège de France,Paris[3],
Ecole Polytechnique,Palaiseau[4]-Laboratoire de l'Accélérateur Linéaire,Orsay[5]

J. Badier[4], J. Boucrot[5], G. Burgun[1], O. Callot[5], Ph. Charpentier[1], M. Crozon[3], D. Decamp[2], P. Delpierre[3], A. Diop[3], R. Dubé[5], B. Gandois[1], R. Hagelberg[2], M. Hansroul[2], W. Kienzle[2], A. Lafontaine[1], P. Le Dû[1], J. Lefrançois[5], Th. Leray[3], G. Matthiae[2], A. Michelini[2], Ph. Miné[4], H. Nguyen Ngnoc[5], O. Runolfsson[2], P. Siegrist[1], J. Timmermans[2], J. Valentin[3], R. Vanderhaghen[4], S. Weisz[2].

ABSTRACT

We have studied vector meson production by a tagged ($\pi^{\pm}$, $K^{\pm}$, $p^{\pm}$) 200 GeV/c beam through their μ pair decay mode. We report here on the production of low mass resonances (ρ^0, ω, ϕ) at high transverse momentum, on J/ψ production and its x, p_t and cosθ distributions. We give also the first evidence for T production by 200 and 280 GeV/c pions.

EPS International Conference on High Energy Physics
Geneva, 27 June - 4 July 1979

1. INTRODUCTION

We have measured μ pair production by $\pi^{\pm}$, $K^{\pm}$ and $p^{\pm}$ simultaneously on hydrogen and platinum using the large acceptance spectrometer of the CERN NA3 experiment. This is an inclusive experiment, as all hadrons are dumped in an iron shield 40 cm downstream from the platinum target (a conical uranium plug of 30 mrad dumps the residual incident beam). The set-up configuration shown in fig. 1 is described elsewhere[1,2].

We have used the secondary beam H8 of CERN SPS, at two beam momenta : 200 GeV/c and 280 GeV/c.

For the negative beam, identification of minority particles (K^- and $\bar{p}$) is provided by two CEDAR's[3] (Differential Cerenkov Counters), identifying K^-'s, and $\bar{p}$'s respectively.

For the positive beam, π^+'s are identified by two threshold Cerenkov counters, K^+'s by the two CEDAR's. Contents of the negative and positive beams are given in table 1.

All Cerenkov counters timings are recorded onto tape via a TDC, in order to compute contamination, electronics dead time and inefficiencies.

The large acceptance of our apparatus allows us to observe production of resonances decaying into $\mu^+\mu^-$ pairs, from $\rho^0(780)$ up to the T(9460) family.

In this paper, we present the analysis of resonance production in the 3 following sections :

sect. 2 : low mass resonances - ρ^0, ω, ϕ
sect. 3 : intermediate mass region - J/ψ
sect. 4 : high mass region - T family

2. LOW MASS RESONANCES

At small values of p_t, our trigger[1] is quite inefficient for such low masses (less than 5% for $p_t < 1.5$ GeV/c). This is due to the fact that we require at least one muon of p_t larger than 1.0 GeV/c or two muons, each with p_t larger than 0.7 GeV/c.

For this reason, we concentrated our study on muon pairs of p_t greater than 2.0 GeV/c for masses between 0.4 and 2.0 GeV/c^2. Fig. 2 shows the mass spectra for incident π^+'s and K^+'s(*).

(*) Background from π decays are estimated from like sign pairs to be less than 1% for p_t larger than 2 GeV/c.

2.1 Comparison of ρ^0, ω and ϕ production

We have fitted our mass spectra using the following assumptions :

(a) a $\mu^+\mu^-$ continuum parametrized as $e^{-M/\lambda}$

(b) three resonances : ρ^0, ω, ϕ assuming $m_\rho = m_\omega$, a natural width of 155 MeV for ρ^0, no interference between ρ^0 and ω, the same resolution δ for each resonance, and equal cross sections for ρ^0 and ω production.

As a first step, we use $m\rho$, m_ϕ, δ, λ, $R_{\phi\rho}$ and the fraction of continuum as free parameters, with

$$R_{\phi\rho} \equiv B\sigma(\phi)/B\sigma(\rho^0)$$

The result of this fit for incident π^+'s is given in table 2. In a second step we have fixed the resonance masses to their canonical value, and, for kaon induced spectra, we have fixed the resolution (δ) to be 108 MeV/c^2, which is the mean value of π^+ and π^- induced spectra.

Table 3 gives the results of these fits, for incident $\pi^\pm$, $K^\pm$ and protons. This table gives also the cross section ratio of ϕ relative to ρ^0, taking into account $\mu^+\mu^-$ branching ratios from e^+e^- annihilation, i.e.

$$\frac{B(\phi \to \mu^+\mu^-)}{B(\rho^0 \to \mu^+\mu^-)} = 7.21 \pm 0.87$$

One can see that the production of ϕ relative to ρ^0 is about two times larger for kaons than for pions or protons. This is qualitatively expected from quark contents, as kaons have strange valence quarks.

But the production ratio of ϕ produced by pions over ρ^0 produced by pions does not seem to decrease as p_t increases, as would be expected from a quark scattering model.

2.2 Cross section and P_t dependance

Using the relative composition of our beam (known from CEDAR's to about 10%), we can calculate ratios of cross sections for different incident particles, independently of acceptance corrections (if p_t distributions are not too different). They are reported in table 4.

For $p_t > 2$ GeV/c, our acceptance is around 10%, increasing with p_t. p_t differential cross sections are shown in fig. 3 for a mass interval from

0.6 to 1.0 GeV/c^2 for incident π^+, π^- and protons. Only statistical errors are shown. Systematic errors on normalisation, acceptance, etc. are estimated to about 20%.

The P_t distribution is well fitted by a parametrisation of the form

$$\frac{1}{p_t}\frac{d}{dp_t} \propto e^{-(3.2 \pm 0.2)p_t}$$

This slope value, as well as the absolute cross section are in good agreement with Anderson et al[4] who measured ρ^0 and ω production by 150 GeV/c pions and protons for p_t smaller than 2 GeV/c.

3. J/ψ PRODUCTION

We have observed a large sample of J/ψ events (fig. 4) in their dimuon decay mode.

Table 5 gives our actual statistics for all incident particles and both targets (hydrogen and platinum)

3.1 Comparison of J/ψ production by π^+ and π^- on protons

We have used our data on both hydrogen and platinum targets. From the number of events on each target, we can deduce two ratios R_{π^+} and R_{π^-} which are independant of absolute normalisation, as both targets are used simultaneously.

$$R_{\pi^-} \equiv \left(\frac{\psi H_2}{\psi Pt}\right)_{\pi^-} = 0.0209 \qquad R_{\pi^+} \equiv \left(\frac{\psi H_2}{\psi Pt}\right)_{\pi^+} = 0.0205$$

The ratio $R \equiv \dfrac{R_{\pi^+}}{R_{\pi^-}}$ is then independant of acceptance corrections.

One gets $R = 0.98 \pm 0.03$

Let us call : $\sigma_+ \equiv \sigma(\pi^+ p \to \psi) = \sigma(\pi^- n \to \psi)$

$\sigma_- \equiv \sigma(\pi^- p \to \psi) = \sigma(\pi^+ n \to \psi)$

If $\alpha = 0.6$ is the fraction of neutrons in the platinum target, the ratio R can be written as

$$R = \frac{\sigma_+}{A(\alpha\sigma_- + (1-\alpha)\sigma_+)} \Big/ \frac{\sigma_-}{A((1-\alpha)\sigma_- + \alpha\sigma_+)} \qquad (3.1)$$

This equation allows to determine the ratio

$$r_{H_2} = \frac{\sigma_+}{\sigma_-} = 0.987 \pm 0.02 \qquad (3.2)$$

which implies

$$r_{Pt} = \frac{\sigma(\pi^+ Pt \to \psi)}{\sigma(\pi^- Pt \to \psi)} = 1.003 \pm 0.004 \qquad (3.3)$$

The errors given here are statistical only, we estimate the systematic error to be less than 5% on r_{H_2} and 1% on r_{Pt}.

3.2 Total cross section and A dependence

The total cross section and the cross section for $x \geq 0$ have been evaluated from a clean sample of our J/ψ events, for incident π^-'s of 200 GeV/c and 280 GeV/c. They have been corrected for reinteraction in the platinum target, measured to be 10% at 200 GeV/c in a 6 cm target, and 19% at 280 GeV/c in a 11 cm target.

Relative cross sections for other particles have been determined from CEDAR's information (they are known to about 10%). Calibration between positive and negative beams is made using equation 3.3 . The cross sections are given in table 6.

Combining the data obtained on hydrogen and platinum targets, we may estimate the mass dependence of J/ψ production.

Experimentally, the ratio

$$\frac{A\,\sigma(\pi^- H_2 \to J/\psi)}{\sigma(\pi^- Pt \to J/\psi)}$$ is equal to 1.31 ± 0.18

Assuming for the A dependance the power law A^α, we get

$$\alpha = 0.95 \pm 0.03$$

In table 7 we recall the earlier measurements of α from incident pions. Using our measured value of α, we have plotted in fig. 5

$M^2\ \sigma_{tot}\ (\pi^- N \to J/\psi)$ as a function of $M/\sqrt{s}$ for different experiments.

3.3 x distribution of J/ψ

In what follows x is defined to be $x \equiv 2P_L^*/\sqrt{s}$, where P_L^* is the longitudinal momentum of the dimuon in the center of mass frame of the reaction, $\sqrt{s}$ the total energy.

Fig. 6 shows the acceptance of our apparatus as a function of x and the differential cross section $d\sigma/dx$ of π^- induced J/ψ events. The acceptance is calculated by a Monte-Carlo program, assuming an isotropic decay distribution of the muons in the J/ψ rest frame (see sect. 3.5) In fig. 7 we give the ratio :

$$R_X(x) = \frac{d\sigma/dx\ (XPt \to J/\psi)}{d\sigma/dx\ (\pi^{\pm}Pt \to J/\psi)}$$

The relative normalisation of positive and negative beams is made using the result of equation (3.3), i.e.

$$\sigma(\pi^+Pt \to J/\psi) = \sigma(\pi^-Pt \to J/\psi) \quad \text{(within 1\%)}$$

The normalisation of $K^{\pm}$, $\bar{p}$ and protons are known within 10%. Error bars do not include this systematic error. The x distribution of all meson induced reactions are similar. Those of the baryons induced reactions show a steep fall off with x, similar for p and $\bar{p}$. At large $x(x \geqslant 0.1)$, $R_p(x)$ has been fitted by $(1 - x)^{2.45\pm0.07}$. The π^- induced distribution has been fitted to a form $(1 - x)^n$ for $x \geqslant 0.2$. The resulting best estimate for n is : $n = 2.98 \pm 0.03$.

The ratio of proton induced to pion induced cross section can easily be interpreted as the ratio of constituents distributions in protons and in pions, falling as $(1 - x)^m$ (from structure functions), with m between 2 and 3.

3.4 p_t distribution of J/ψ

p_t acceptance for J/ψ particles is given in fig. 8 from our Monte-Carlo calculation.

Differential cross sections $1/p_t\ d\sigma/dp_t\ (\pi^- Pt \to J/\psi)$ are shown in

fig. 9 at 200 GeV/c and 280 GeV/c incident momentum.

These cross sections are not well fitted above 4 GeV/c by a function of the form $(1 + p_t^2/m^2)^{-6}$ as was previously reported[7,10] neither with a simple gaussian :

$$e^{-p_t^2/a^2}$$

We have fitted these distributions to a form

$$\frac{1}{p_t}\frac{d\sigma}{dp_t} \propto (1 - x_t)^{\gamma} \left(1 + \frac{p_t^2}{m^2}\right)^{\beta} \quad \text{where} \quad x_t \equiv \frac{2p_t}{\sqrt{s}}$$

γ has first been determined by a least square fit to the ratio of the two p_t distributions. We find γ to be

$$\gamma = 5.56 \pm 0.50$$

Fixing m at the mass of the J/ψ, one gets a value of β from a simultaneous fit of 200 and 280 GeV/c data :

$$\beta = -4.86 \pm 0.02$$

with a χ^2 of 153 for 123 degrees of freedom.

The resulting curves are shown in fig. 9.

Leaving m as a free parameter leads to the result

$$\beta = -6.01 \pm 0.13$$
$$m = 3.66 \pm 0.10 \text{ GeV/c}^2$$

and the χ^2 becomes 106 for 122 degrees of freedom.

A summary of the results for the average values $< p_t >$ and $< p_t^2 >$ is given in table 8.

3.5 Angular distribution of muons

The study of angular distribution of muons in the J/ψ rest frame gives information about production mechanism of J/ψ. The choice of the axis depends on the production model. In the Gottfried-Jackson frame, for example, the angular distribution is of the form

$$\frac{d\sigma}{d\ \cos\theta_{GJ}} = A\ (1 + \lambda\cos^2\theta_{GJ}) \quad . \qquad (3.4)$$

In a quark fusion model producing directly the J/ψ, λ is given by[7]

$$\lambda = \frac{1 - 4m^2/Q^2}{1 + 4m^2/Q^2} \qquad (3.5)$$

The cross section as a function of the Godfried-Jackson angle is given in fig. 10 for incident 200 GeV/c π^-'s, in the mass range 2.7 to 3.5 GeV/c^2

A fit of λ gives $\lambda = 0.12 \pm 0.05$. If we substract the (9±2%) continuum contribution ($\lambda = 0.8 \pm 0.2$)[13], one gets $\lambda = 0.05 \pm 0.07$, in very good agreement with ref.(7) and (11).

This isotropic distribution has been used in calculating the acceptance for x and P_t at the J/ψ, and shows that, for J/ψ, the choice of the reference axis is not crucial, as all axes would give the same result.

This result is not in contradiction with heavy quark fusion, (from) equation 3.5) nor with a model of gluons or light quark fusion producing first a χ resonance decaying into J/ψ + γ.

4. T RESONANCES

Our data show in the dimuon mass spectrum a clear signal around 9.5 GeV/c^2 in π^+Pt interactions, as well as, when cumulating events from the platinum target and from the uranium dump (fig. 11). This is the first evidence for T production[12] in pion induced reactions. This signal is sharper for incident π^+'s than for π^-'s, as Drell-Yan continuum falls steeper for π^+'s (fig. 12)[13]. From fig. 12, one can estimate that, at 9.5 GeV/c^2, the continuum ratio is about 1/3. If we assume equal T cross sections for π^+ and π^-, we would expect a signal to Drell-Yan ratio 3 times larger for incident π^+'s than for π^-'s.

4.1 Fit of T resonances

The resolution at 9.5 GeV/c^2 has been evaluated by Monte-Carlo to be around 4.5% at 200 GeV/c and 5% at 280 GeV/c (dominated by momentum resolution)

Due to this poor resolution, masses of T resonances have been fixed

at their well known values[15].

Acceptance for Υ has been calculated assuming, as for the J/ψ, an isotropic decay distribution of muons in Υ rest frame, and for Drell-Yan continuum a $(1 + \cos^2\theta_{GJ})$ dependence in Godfried-Jackson frame, compatible with our data[13].

Dimuon mass spectra (fig. 13) have been fitted for $M > 4.3$ GeV/c^2 at 200 GeV/c and $M > 4.5$ GeV/c^2 at 280 GeV/c. The Drell-Yan continuum is parametrized as $1/\lambda\ e^{-M/\lambda}$.

Three resonances have been added, letting free four parameters :

i) the ratio α of all resonances to Drell-Yan at 9.46 GeV/c^2

$$\alpha = \frac{\sigma_{tot}\ (\pi Pt \to \Upsilon, \Upsilon', \Upsilon'')}{d\sigma/dM(\pi Pt \to \text{Drell-Yan at } 9.46\ \text{GeV}/c^2)}$$

ii) the abundance of $\Upsilon'$and Υ'' relative to Υ : α_1 and α_2

iii) λ, the Drell-Yan slope

Because of our resolution, α_1 and α_2 are badly measured, but due to the low statistics, they have to be left free to determine the number of Υ events.

The results of these fits are given in table 9, as well as the number of Υ's actually observed, as given by the fit. We have considered here not only the events from our main heavy target (platinum), but also from the uranium beam dump.

4.2 Production cross section

From table 9 one can evaluate the cross section ratio of Υ production to J/ψ production. This ratio is reported in table 10.

4.3 Υ production from K^+'s and protons

A fit of mass spectra for incident K^+'s and protons above 4.5 GeV/c on both the platinum target and the uranium dump gives for cross section relative to incident π^+'s :

$$\frac{\sigma(K^+Pt \to T)}{\sigma(\pi^+Pt \to T)} = 0.34 \pm 0.23$$

$$\frac{\sigma(pPt \to T)}{\sigma(\pi^+Pt \to T)} = 0.03 \pm 0.02$$

Let us recall that we get from table 10 :

$$\frac{\sigma(\pi^-Pt \to T)}{\sigma(\pi^+Pt \to T)} = 0.76 \pm 0.29$$

A quark fusion model would give, using the structure functions obtained from our Drell-Yan analysis[1] the predictions :

$$\frac{\sigma(\pi^-Pt \to T)}{\sigma(\pi^+Pt \to T)} \simeq 0.83$$

$$\frac{\sigma(K^+Pt \to T)}{\sigma(\pi^+Pt \to T)} \simeq 0.10$$

$$\frac{\sigma(pPt \to T)}{\sigma(\pi^+Pt \to T)} \simeq 0.05$$

The experimental results are in agreement with these predictions. Let us remark that a gluon fusion model would give the same cross section for K^+ and π^+, which is excluded by the data. Our data give for 200 GeV/c protons a cross section

$$B\sigma\,(pPt \to T) = 5.4 \pm 4.5 \quad 10^{-38}\,cm^2/nucleon,$$

assuming a linear A dependence.

Assuming a flat y distribution, between the kinematics limits, one gets

$$B\,\frac{d\sigma}{dy}\Big|_{y\,=\,0} = 4.5 \pm 3.8 \quad 10^{-38}\,cm^2$$

This result is compared in fig. 14 to the existing measurements (from ref. 16) Our result is in good agreement with an exponential eye fit of the $\sqrt{\tau}$ dependence given on fig. 14 (the points from Yoh et al[10] are not measured at $y = 0$, but at $y = \langle y \rangle_{acc}$, mean value of y for the acceptance of their apparatus, i.e. $y = 0.2$ at 300 GeV/c and $y = 0.4$ at 200 GeV/c)

5. CONCLUSIONS

We have measured with large statistics low mass resonances at high transverse momentum, as well as J/ψ production up to 6 GeV/c of transverse momentum.

We have also observed the first evidence for Υ production by pions at 200 GeV/c and 280 GeV/c.

For J/ψ production , the following remarks can be made :

(a) π^+ and π^- cross sections on hydrogen are found to be in the ratio 0.987 ± 0.020, giving a cross section ratio on platinum of 1.003 ± 0.004, compatible with a value of 1.

(b) x distributions show a strong difference between incident mesons and baryons, the latter falling more rapidly when x increases. Proton over pion differential cross section falls approximately as $(1 - x)^{2.4}$

(c) p_t distributions are well fitted for 200 and 280 GeV/c by an expression of the form

$$(1 - x_t)^{5.56 \pm 0.50} \; (m_t/m)^{-9.72 \pm 0.04}$$

up to 6 GeV/c.

(d) J/ψ decay distribution is consistent with being isotropic, with a value of λ, from

$$\frac{d\sigma}{d \cos\theta_{GJ}} \propto 1 + \cos^2\theta_{GJ} \quad : \lambda = 0.05 \pm 0.07$$

(e) cross sections have been compared for six different incident particles at the same energy. The ratio of antiproton to proton J/ψ production equals 1.4 ± 0.2, indicating that part of the J/ψ is due to valence quark interactions.

For Υ production, we have determined the ratio to the J/ψ cross section for incident π^+'s and π^-'s at 200 GeV/c and 280 GeV/c to be approximately 2.10^{-4}. This means that Υ production is almost equal for incident π^+'s and π^-'s, and that this production does not vary too fast with beam energy between 200 and 280 GeV/c.

REFERENCES

(1) J. Badier et al., "Experimental determination of the pion and nucleon structure functions by measuring high-mass muon pairs produced by pions of 200 and 280 GeV/c", International Conference on High Energy Physics, Geneva 1979.

(2) J. Badier et al., NA3 spectrometer, paper in preparation, to be published in Nucl. Instr. and Methods.

(3) C. Bovet et al., CERN-SPS/EPP/77.19.

(4) K.J. Anderson et al., Phys. Rev. Letters 37 (1976) 799.

(5) K.J. Anderson et al., Phys. Rev. Letters 42 (1979) 944.

(6) Y.M. Antipov et al., Phys. Letters 76B (1978) 235.

(7) M.A. Abolins et al., Preprint DPHPE 78-05.
M.A. Abolins et al., Phys. Letters 82B (1979) 145.

(8) Y.B. Bushnin et al., Phys. Letters 72B (1977) 269.

(9) M.J. Corden et al., Phys. Letters 68B (1977) 96.

(10) J.K. Yoh et al., Phys. Rev. Letters 41 (1978) 684.
for J/ψ Pt dependence see also
C. Newman, Ph. D. Thesis, University of Chicago 1979, unpublished.

(11) J.G. Branson et al., Phys. Rev. Letters 38 (1977) 1331.

(12) S.W. Herb et al., Phys. Rev. Letters 39 (1977) 252.

(13) J. Badier et al., "Muon pair production above 4 GeV (Drell-Yan continuum) by $\pi^{\pm}$, $K^{\pm}$, $\bar{p}$ and p at 200 GeV/c and by π^{-} at 280 GeV/c on platinum and hydrogen targets", International Conference on High Energy Physics, Geneva 1979.

(14) K. Ueno et al., Fermilab preprint 78/96 (submitted to Phys. Rev. Letters).

(15) J.K. Bienlein et al., Phys. Letters 78B (1978) 360.
C.W. Darden et al., Phys. Letters 78B (1978) 364.

(16) I. Mannelli, "Electron pairs production at the ISR", Proc. 19th Int. Conf. on High Energy Physics, Tokyo 1978.

Table 1

Beam content

P beam	-200 GeV/c	+200 GeV/c
π	96.3%	36%(*)
K	3.1%	4.6%
p	0.62%	59.4%

(*) : a 2m polyethylene absorber placed in the beam has been used to increase the fraction of π^+ from 20% to 36%.

Table 2

Fitted parameters for π^+ induced muon pairs of $p_t > 2.0$ GeV/c and masses between 0.4 and 2.0 GeV/c^2

Parameter	λ(GeV/c^2)	m_ρ(MeV/c^2)	m_ϕ(MeV/c^2)	δ(MeV/c^2)	$R_{\phi\rho}$	χ^2/D.F.
Value	0.661±0.016	791.8±3.5	1037±6	109.5±3.0	0.86±0.04	37.5/33

Table 3

Fitted parameters of mass spectra for 200 GeV/c $\pi^{\pm}$, $K^{\pm}$ and protons in the ρ^0, ω, ϕ region for different P_t ranges

Particle	π^+		K^+	K^-	π^-		proton	
$P_t \rightarrow$	$\geq$ 2.	$\geq$ 3.	$\geq$ 2.	$\geq$ 2.	$\geq$ 2.	$\geq$ 3.	$\geq$ 2.	$\geq$ 3.
λ (GeV/c)	0.687±0.018	.83±0.08	0.67±0.04	0.70±0.09	0.84±0.02	0.74±.04	0.607±.012	0.66±.05
δ (MeV/c^2)	110.5±3.4	108*	108*	108*	106.0±3.0	108*	102.4±2.6	108*
$R_{\phi\rho}$	1.05±0.05	1.33±.16	2.25±0.16	2.46±0.50	1.11±0.04	1.54±.17	0.86±0.03	1.04±.13
χ^2/D.F.	49.8/35	56/36	64/36	33.2/36	53/35	65.7/36	47.3/35	25.2/36
$\sigma(\phi)/\sigma(\rho)$ (%)	14.6±1.9	18.5±3.2	31.2±4.4	34.1±8.1	15.4±2.0	21.4±3.5	11.9±1.5	14.4±2.5

(*) = fixed parameter

Table 4

Cross section for low mass resonances relative to π^- induced reaction for $P_t > 2$ GeV/c (ω and ρ^0 production cross sections have been assumed to be equal).

X	π^+	K^+	K^-	p
$\sigma(XPt \to \rho^0)/\sigma(\pi^- Pt \to \rho)$	1.12 ± 0.07	0.85 ± 0.10	0.94 ± 0.11	1.11 ± 0.13
$\sigma(XPt \to \phi)/\sigma(\pi^- Pt \to \phi)$	1.06 ± 0.07	1.75 ± 0.20	2.11 ± 0.24	0.86 ± 0.10

Table 5

Statistics of J/ψ events

P_{beam}	200 GeV/c			200 GeV/c			280 GeV/c
Part. / Target	π^-	K^-	$\bar{p}$	π^+	K^+	p	π^-
H_2	3,000	56	17	2,200	340	2,300	-
Pt	145,000	2,800	1,000	108,000	16,000	101,000	130,000

Table 6

(a) J/ψ cross sections for π^- at 200 GeV/c and 280 GeV/c in μb/Pt nucleus (A = 195) corrected for reinteractions in the target.

P_{beam}	200 GeV/c	280 GeV/c
part.	π^-	π^-
σ_{tot}	1.56 ± 0.27	2.12 ± 0.47
$\sigma(x > 0)$	0.76 ± 0.14	1.05 ± 0.24

(b) Cross section for all other particles relative to π^-.

P_{beam}	200 GeV/c				
part.	K^-	$\bar{p}$	π^+	K^+	p
$\frac{\sigma_{tot}(X)}{\sigma_{tot}(\pi^-)}$	1.1±0.1	0.83±0.12	1.01±0.02	0.78±0.08	0.59±0.10

Table 7

Measurement of A dependence power α for incident pions.

References	P_{inc}	α	α average
Anderson et al. (5)	225 GeV/c	0.87 ± 0.05	
Antipov et al. (6)	43 GeV/c	0.92 ± 0.06	0.927 ± 0.030
this experiment	200 GeV/c	0.95 ± 0.03	

Table 8

Average values of p_t and p_t^2 for J/ψ events in GeV/c.

P_{beam}	200 GeV/c						280 GeV/c
Part.	π^-	K^-	$\bar{p}$	π^+	K^+	p	π^-
$< p_t >$	1.12 ± 0.01	1.13±0.04	1.05±0.06	1.12 ± 0.01	1.14 ± 0.03	1.07 ± 0.01	1.18 ± 0.01
$< p_t^2 >$	1.70 ± 0.03	1.69±0.10	1.50±0.20	1.66 ± 0.03	1.75 ± 0.10	1.52 ± 0.02	1.86 ± 0.02

Table 9

Fitted parameters of mass spectra of the form :

$$f(M) = 1/\lambda\ e^{-M/\lambda} + \alpha \frac{(T + \alpha_1 T' + \alpha_2 T'')}{1 + \alpha_1 + \alpha_2} \cdot 1/\lambda\ e^{-9.46/\lambda}$$

Particle	π^+ 200 GeV/c		π^- 200 GeV/c		π^- 280 GeV/c	
Target	Pt	Pt + U	Pt	Pt + U	Pt	Pt + U
λ (GeV/c)	0.948±0.026	0.977±0.024	1.100±0.019	1.049±0.016	1.228±0.023	1.158±0.013
α (GeV/c^2)	4.22±0.98	3.38±0.64	0.87±0.26	1.62±0.29	0.70±0.22	1.13±0.16
$N_T + N_T' + N_T''$	53.2±12	103.7±18	54.6±15.5	123.6±21	65.5±20	138.4±18.4

Table 10

Ratio of Υ to J/ψ production times the branching ratio into μ pair, for different incident beams (systematic errors included)

Particle	π^+ 200 GeV/c	π^- 200 GeV/c	π^- 280 GeV/c
$\frac{B\sigma(\Upsilon + \Upsilon' + \Upsilon'')}{B\sigma(J/\psi)}$	$(2.26 \pm 0.56)10^{-4}$	$(1.73 \pm 0.52)10^{-4}$	$(2.07 \pm 0.67)10^{-4}$

Figure captions

Fig. 1 Set-up of NA3 experiment in its μ pair configuration.

Fig. 2 Mass spectrum in the ρ^0, ω, ϕ region with $P_t > 2$ GeV/c for a) Incident π^+, b) Incident K^+.

Fig. 3 $1/p_t \, d\sigma/dp_t$ for masses between 0.6 GeV/c^2 and 1.0 GeV/c^2.

Fig. 4 Mass spectrum for J/ψ events from incident 200 GeV/c π^-'s.

Fig. 5 J/ψ excitation curve for incident pions.

Fig. 6 x acceptance for J/ψ and differential cross section $d\sigma/dx$ for incident π^-'s at J/ψ.

Fig. 7 Ratio of $d\sigma/dx$ for different particles over $d\sigma/dx$ for incident pions. a) Incident mesons b) Incident baryons

Fig. 8 p_t acceptance for J/ψ.

Fig. 9 $1/p_t \, d\sigma/dp_t \, (\pi^- p_t \rightarrow J/\psi)$ for 200 GeV/c and 280 GeV/c pions.

Fig. 10 $d\sigma/d \cos\theta_{GJ}$ for J/ψ events from 200 GeV/c π^-'s.

Fig. 11 dN/dM for incident π^+'s on platinum and platinum + uranium targets.

Fig. 12 $\dfrac{d\sigma/dM(\pi^+ P_t \rightarrow \mu^+\mu^-)}{d\sigma/dM(\pi^- P_t \rightarrow \mu^+\mu^-)}$ as a function of mass (normalised from J/ψ events.)

Fig. 13 dN/dM for incident π^-'s at 200 GeV/c and 280 GeV/c on platinum and platinum + uranium targets.

Fig. 14 $B \left.\dfrac{d\sigma}{dy}\right|_{y=0}$ for proton induced Υ (from ref. 16).

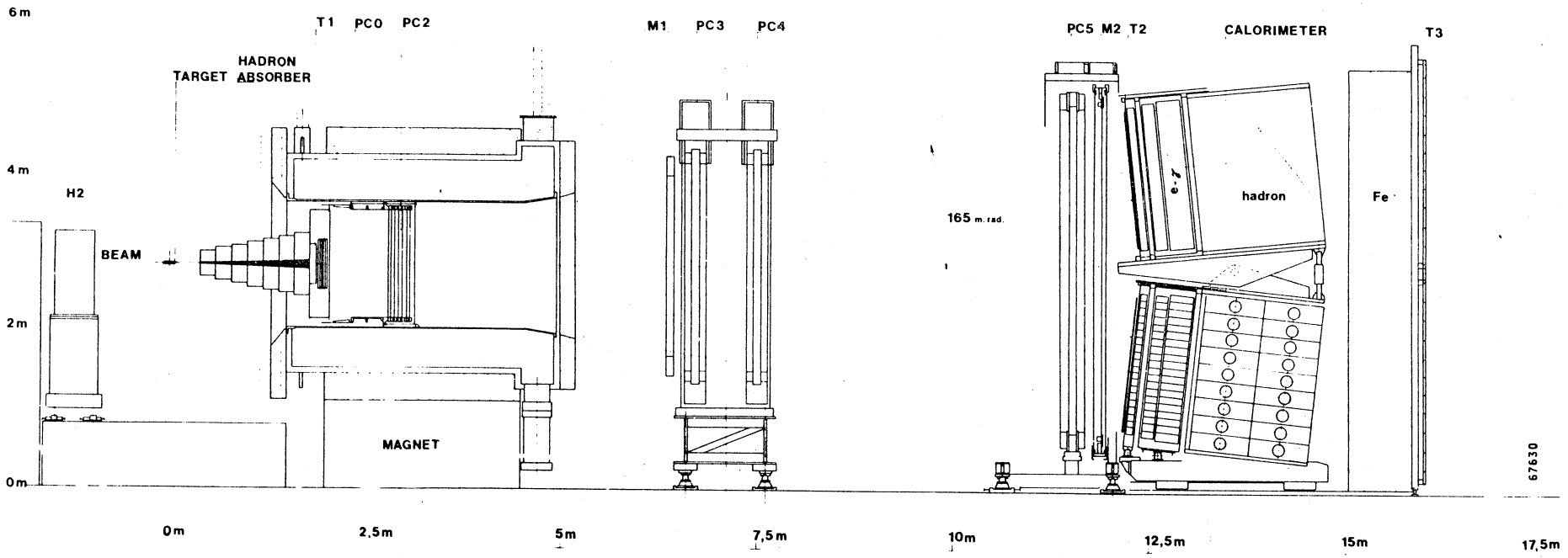
6 m
4 m
2 m
0 m
T1
PC0
PC2
M1
PC3
PC4
PC5
M2
T2
CALORIMETER
T3
HADRON
TARGET
ABSORBER
H2
BEAM
MAGNET
165 m.rad.
e-γ
hadron
Fe
67630
0m
2,5m
5m
7,5m
10m
12,5m
15m
17,5m

FIG. 1

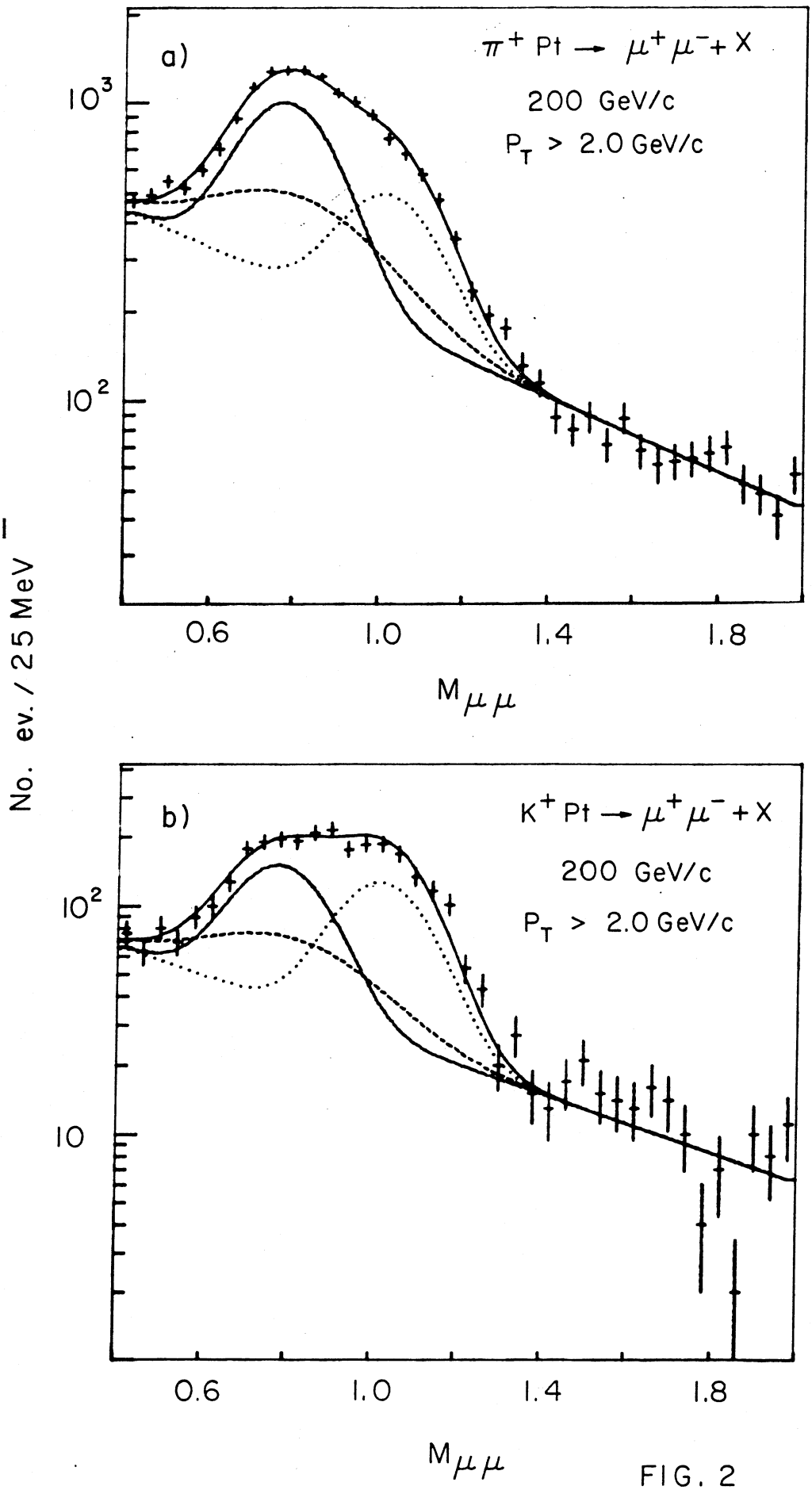
a)
π^+ Pt → $\mu^+\mu^-$ + X
200 GeV/c
P_T > 2.0 GeV/c
10^3
10^2
0.6
1.0
1.4
1.8
$M_{\mu\mu}$
No. ev. / 25 MeV
b)
K^+ Pt → $\mu^+\mu^-$ + X
200 GeV/c
P_T > 2.0 GeV/c
10^2
10
0.6
1.0
1.4
1.8
$M_{\mu\mu}$

FIG. 2

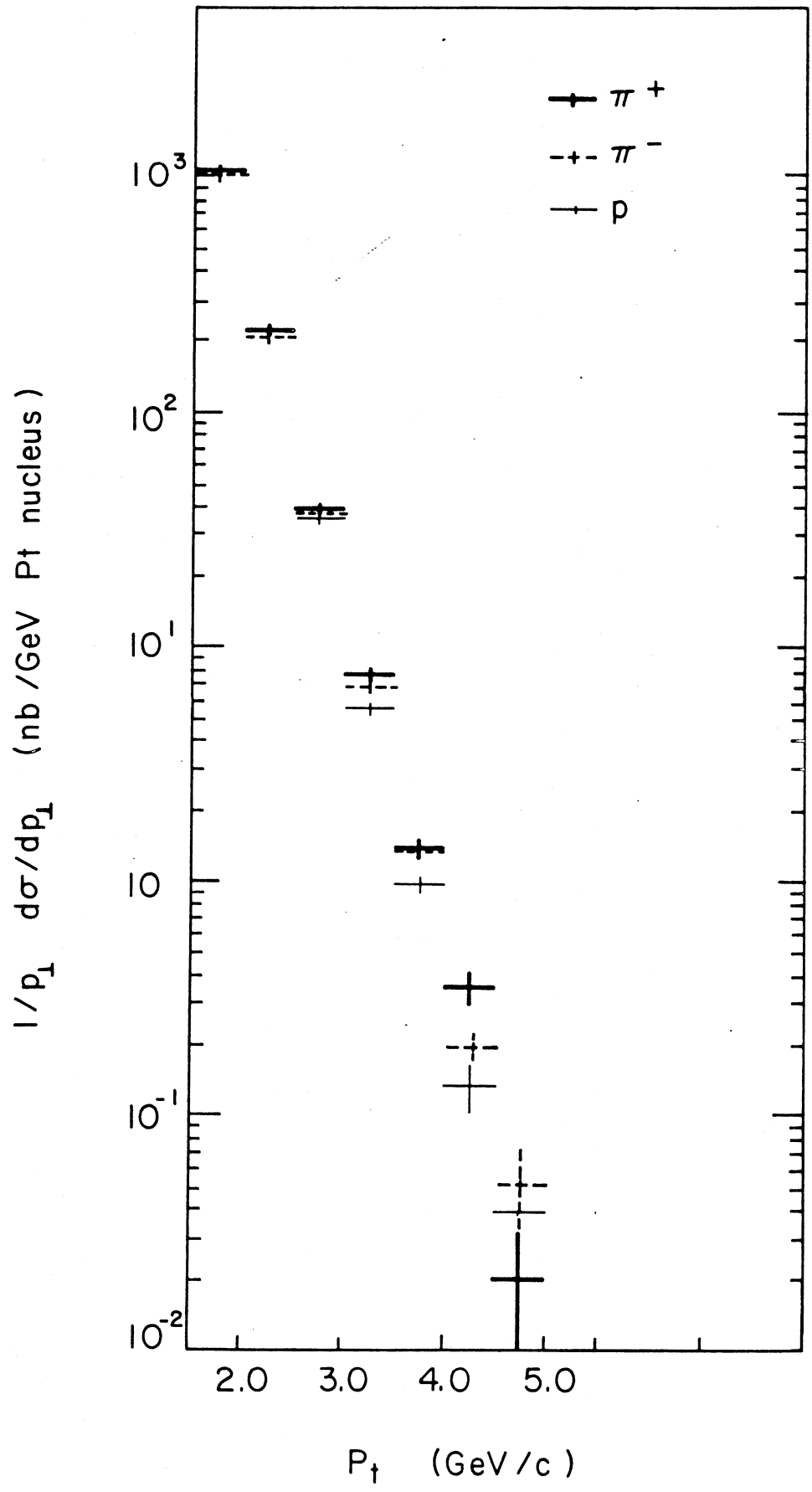
π +
π −
p
10^3
10^2
10^1
10
10^-1
10^-2
2.0
3.0
4.0
5.0
1/p_T dσ/dp_T (nb/GeV Pt nucleus)
P_t (GeV/c)

FIG. 3

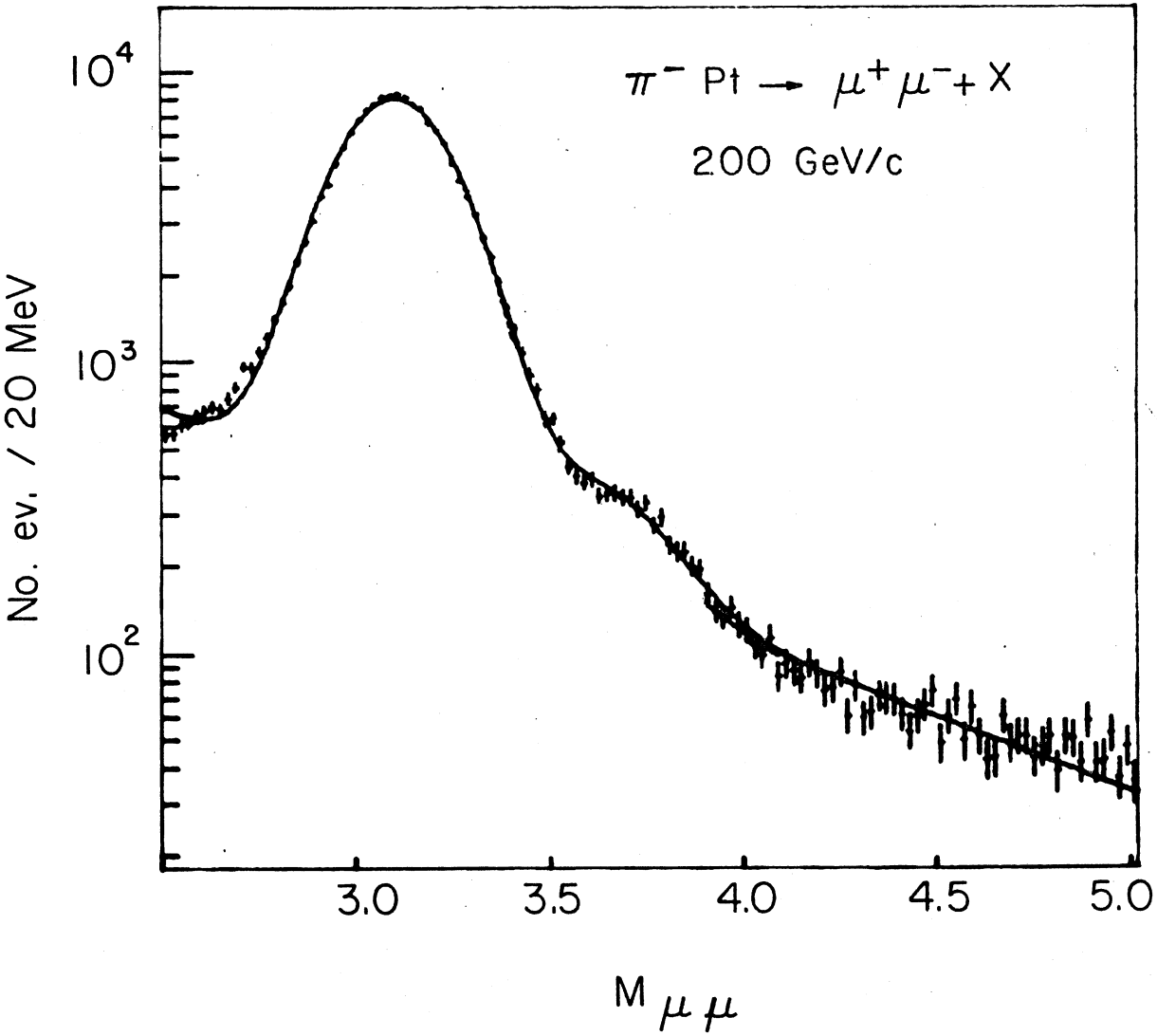

FIG. 4

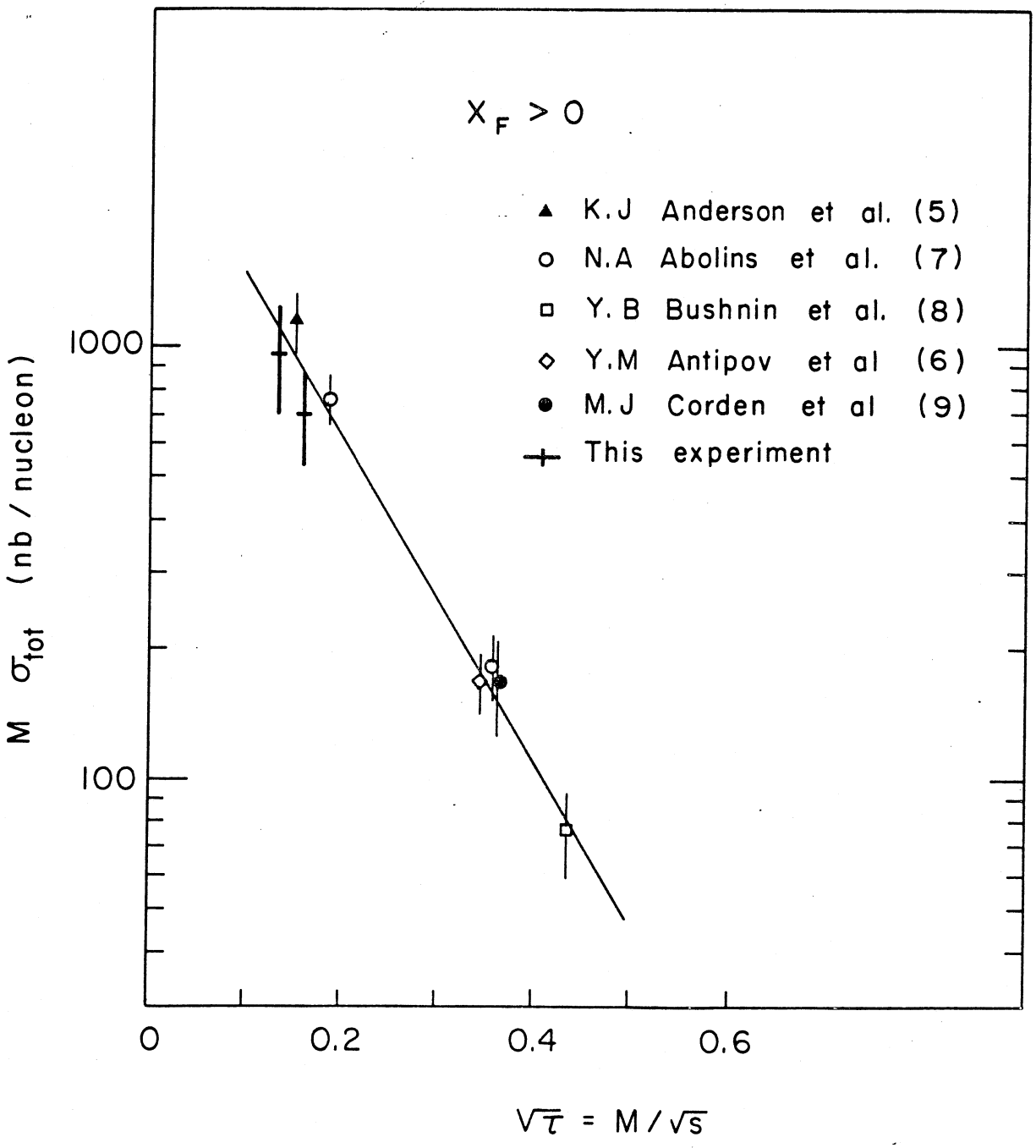
$X_F > 0$
K.J Anderson et al. (5)
N.A Abolins et al. (7)
Y. B Bushnin et al. (8)
Y.M Antipov et al (6)
M.J Corden et al (9)
This experiment
1000
100
M σ_{tot} (nb / nucleon)
0
0.2
0.4
0.6
$\sqrt{\tau} = M/\sqrt{s}$

FIG. 5

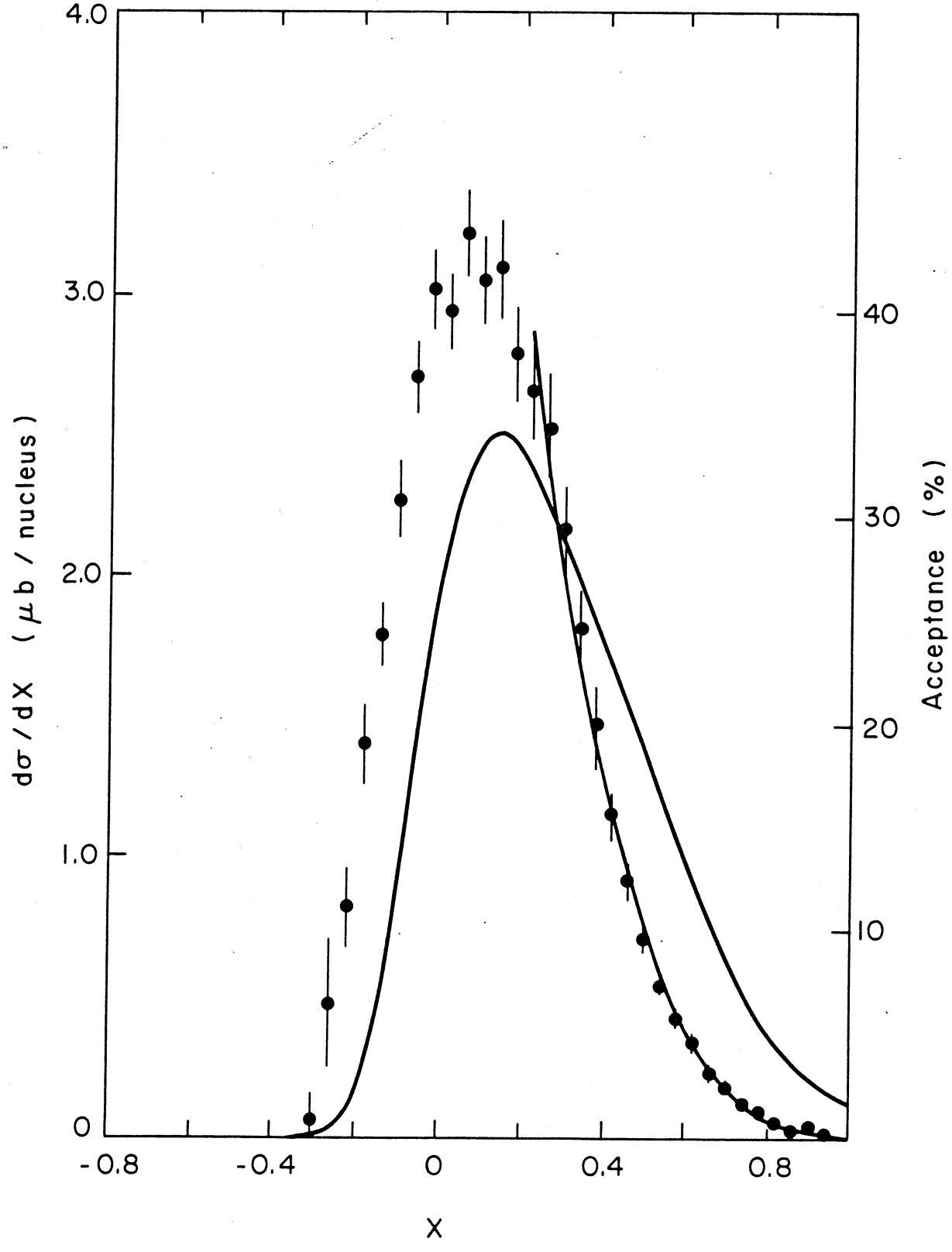
4.0
3.0
2.0
1.0
0
-0.8
-0.4
0
0.4
0.8
X
dσ / dX (μb / nucleus)
40
30
20
10
Acceptance (%)

FIG. 6

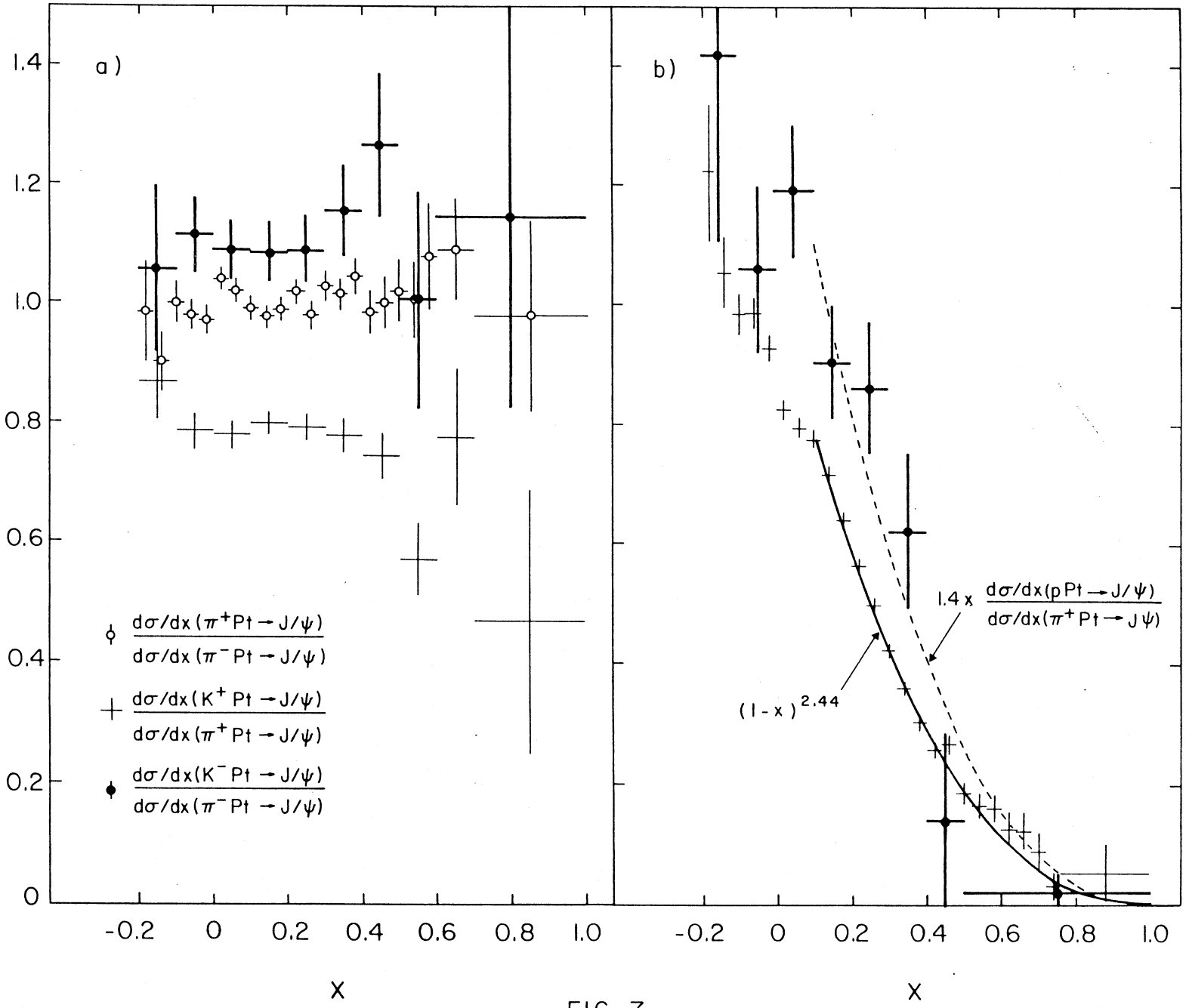
a)
b)
1.4
1.2
1.0
0.8
0.6
0.4
0.2
0
-0.2
0
0.2
0.4
0.6
0.8
1.0
X
$\frac{d\sigma/dx(\pi^+ Pt \to J/\psi)}{d\sigma/dx(\pi^- Pt \to J/\psi)}$
$\frac{d\sigma/dx(K^+ Pt \to J/\psi)}{d\sigma/dx(\pi^+ Pt \to J/\psi)}$
$\frac{d\sigma/dx(K^- Pt \to J/\psi)}{d\sigma/dx(\pi^- Pt \to J/\psi)}$
$1.4 \times \frac{d\sigma/dx(p Pt \to J/\psi)}{d\sigma/dx(\pi^+ Pt \to J\psi)}$
$(1-x)^{2.44}$

FIG. 7

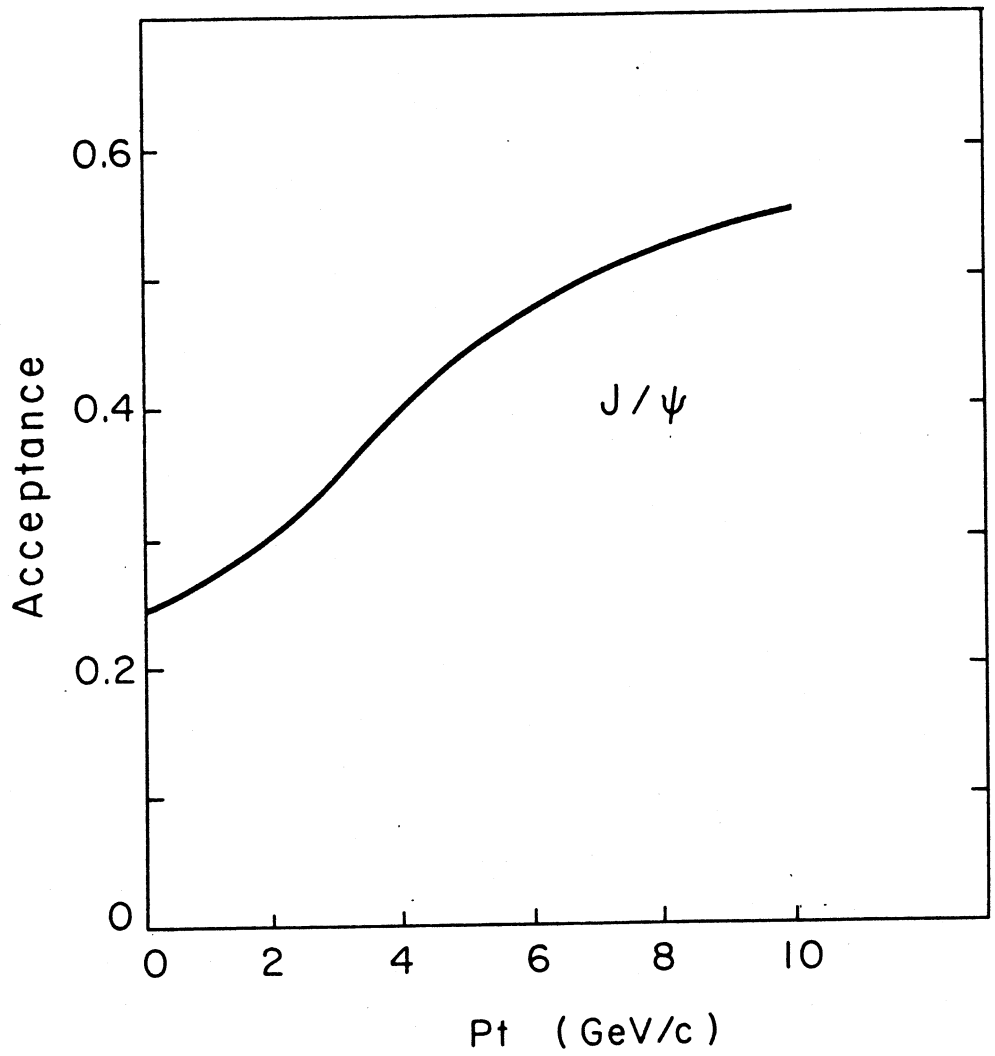

FIG. 8

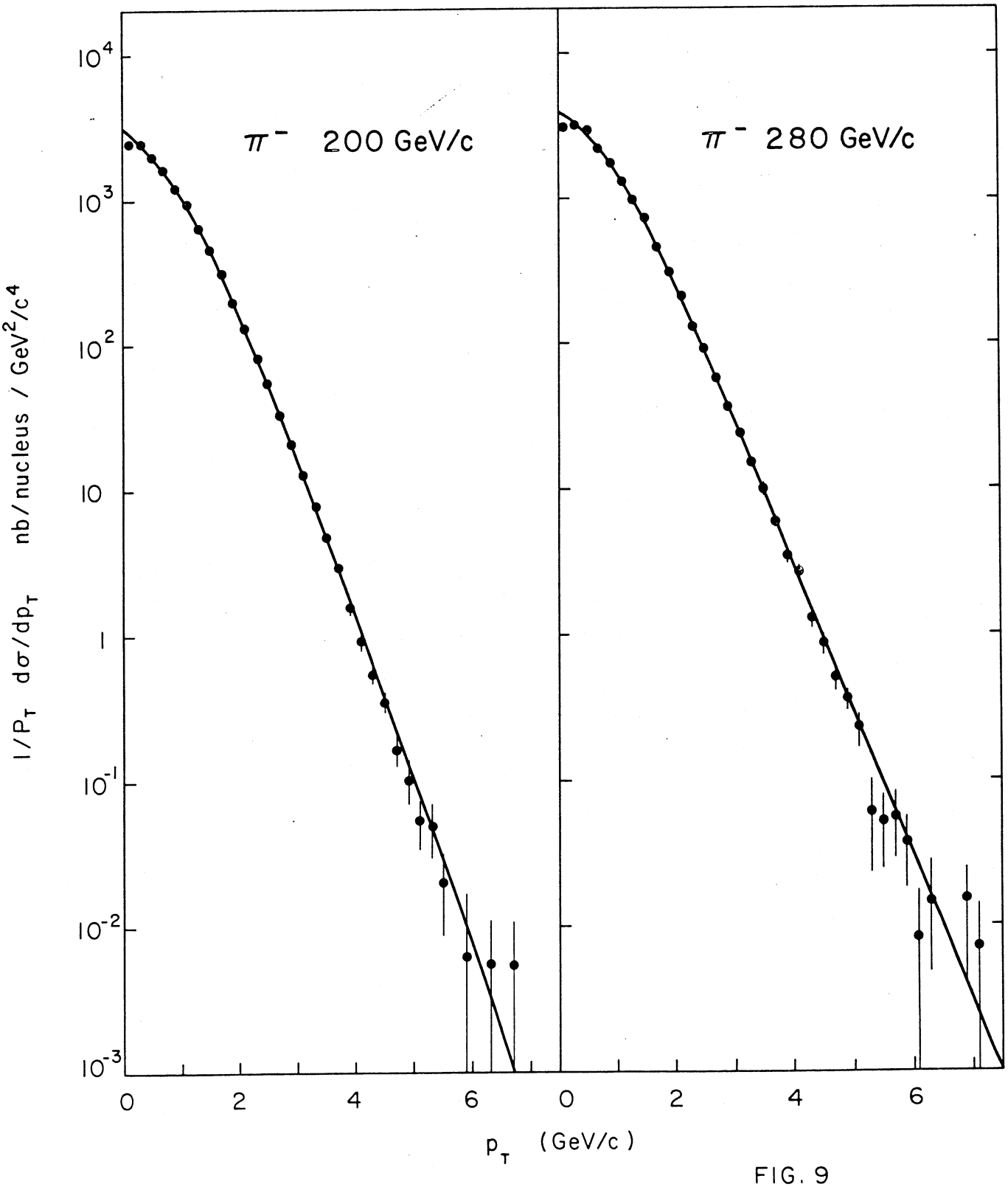
π^- 200 GeV/c
π^- 280 GeV/c
10^4
10^3
10^2
10
1
10^{-1}
10^{-2}
10^{-3}
0
2
4
6
$1/P_T \; d\sigma/dp_T$ nb/nucleus / GeV^2/c^4
p_T (GeV/c)

FIG. 9

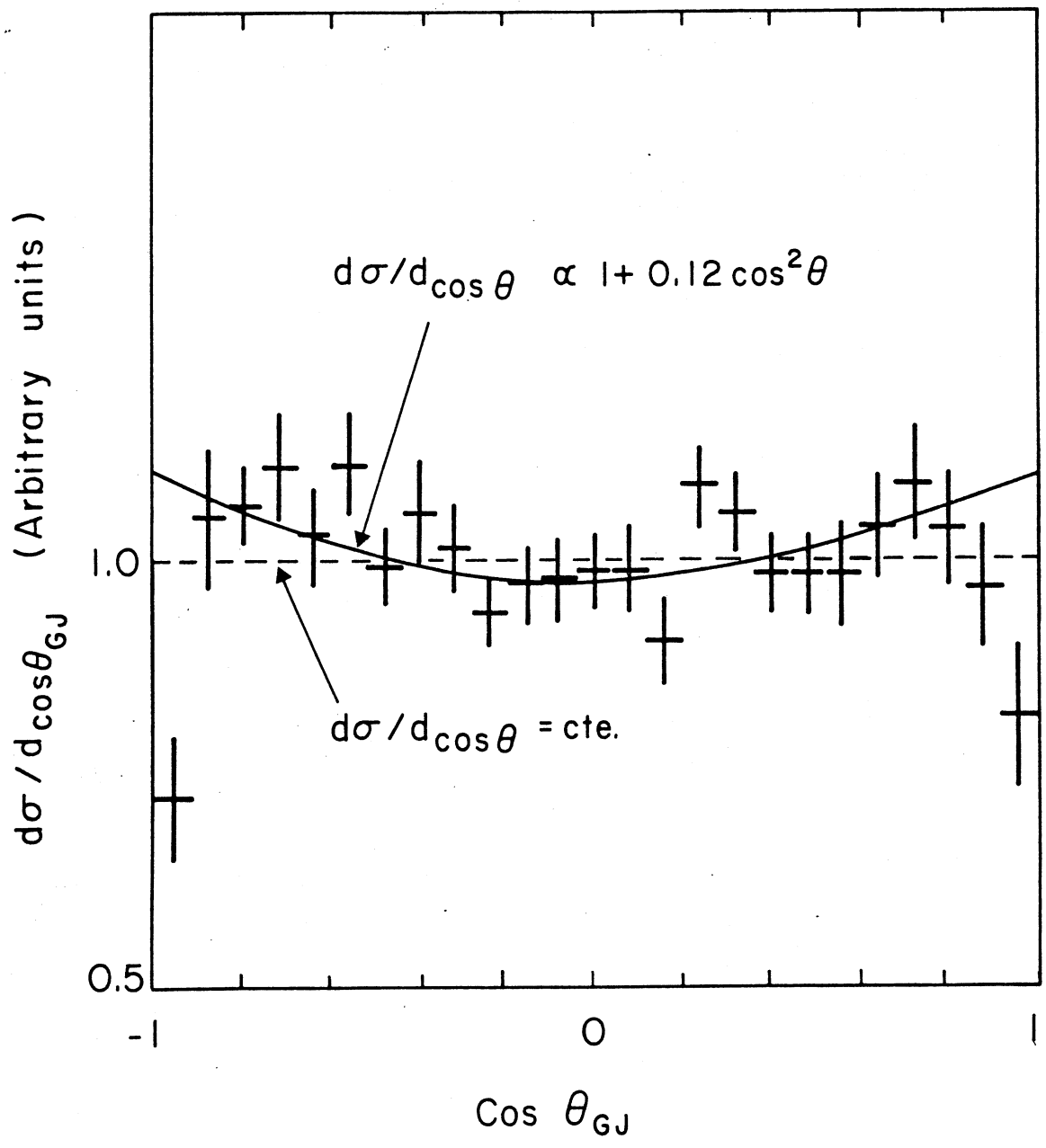
dσ/d cos θ ∝ 1+ 0.12 cos²θ
dσ/d cos θ = cte.
dσ / d cos θ_GJ (Arbitrary units)
1.0
0.5
-1
0
1
Cos θ_GJ

FIG. 10

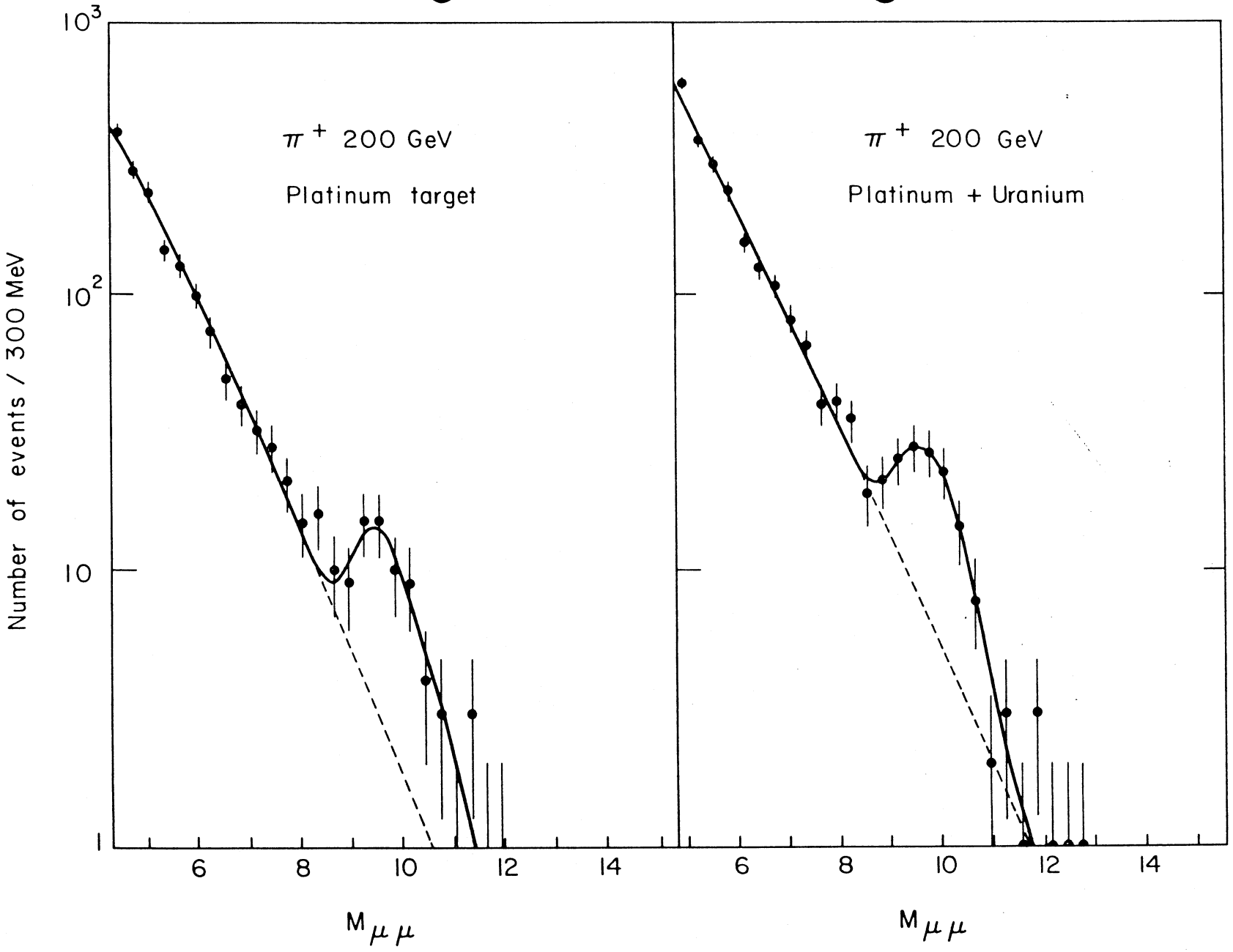
10^3
10^2
10
1
Number of events / 300 MeV
π^+ 200 GeV
Platinum target
π^+ 200 GeV
Platinum + Uranium
6
8
10
12
14
$M_{\mu\mu}$
$M_{\mu\mu}$

FIG. 11

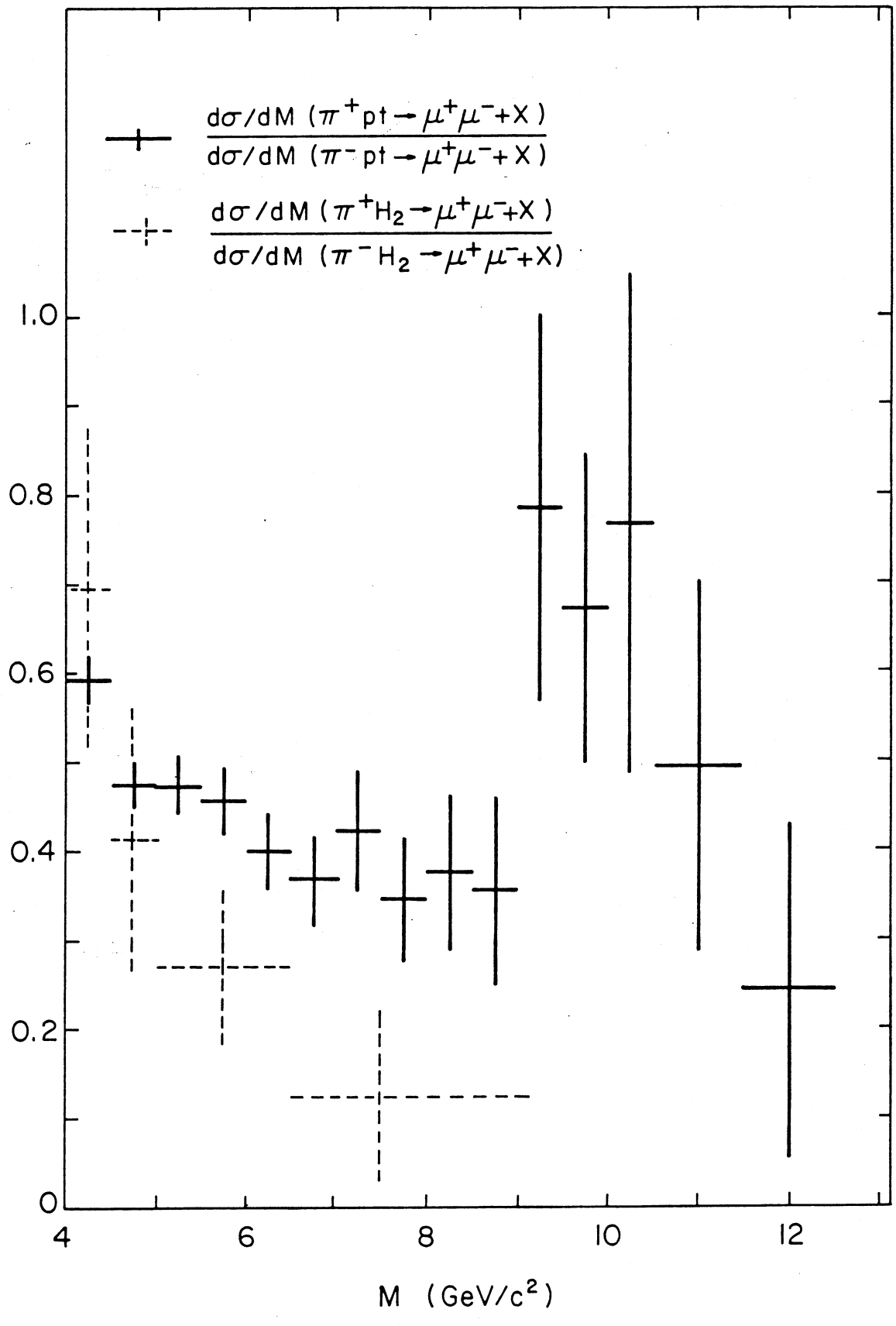
dσ/dM (π⁺pt → μ⁺μ⁻+X)
dσ/dM (π⁻pt → μ⁺μ⁻+X)
dσ/dM (π⁺H₂ → μ⁺μ⁻+X)
dσ/dM (π⁻H₂ → μ⁺μ⁻+X)
1.0
0.8
0.6
0.4
0.2
0
4
6
8
10
12
M (GeV/c²)

FIG. 12

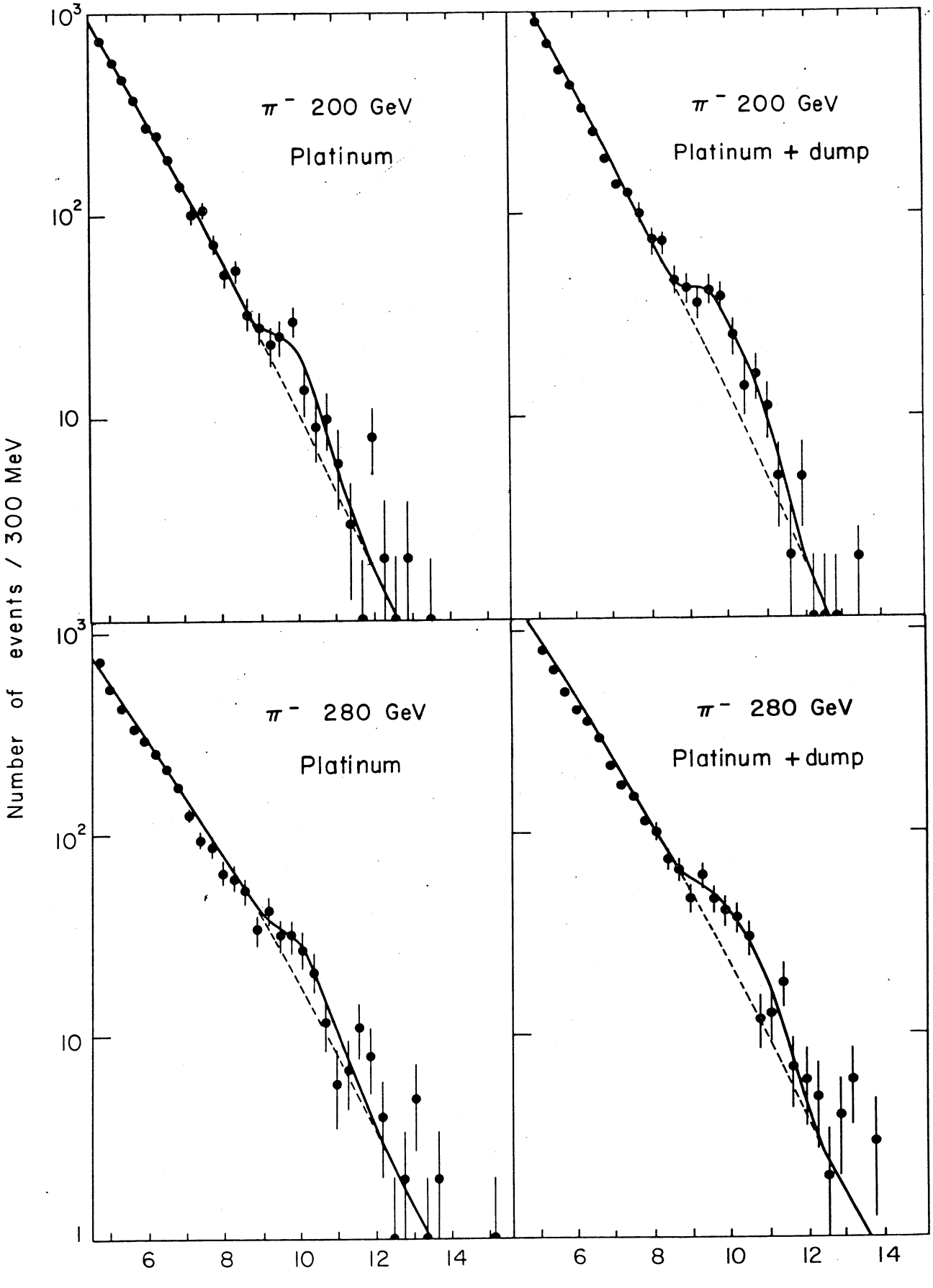
π^- 200 GeV
Platinum
π^- 200 GeV
Platinum + dump
π^- 280 GeV
Platinum
π^- 280 GeV
Platinum + dump
Number of events / 300 MeV
10^3
10^2
10
1
6
8
10
12
14
$M_{\mu\mu}$

FIG. 13

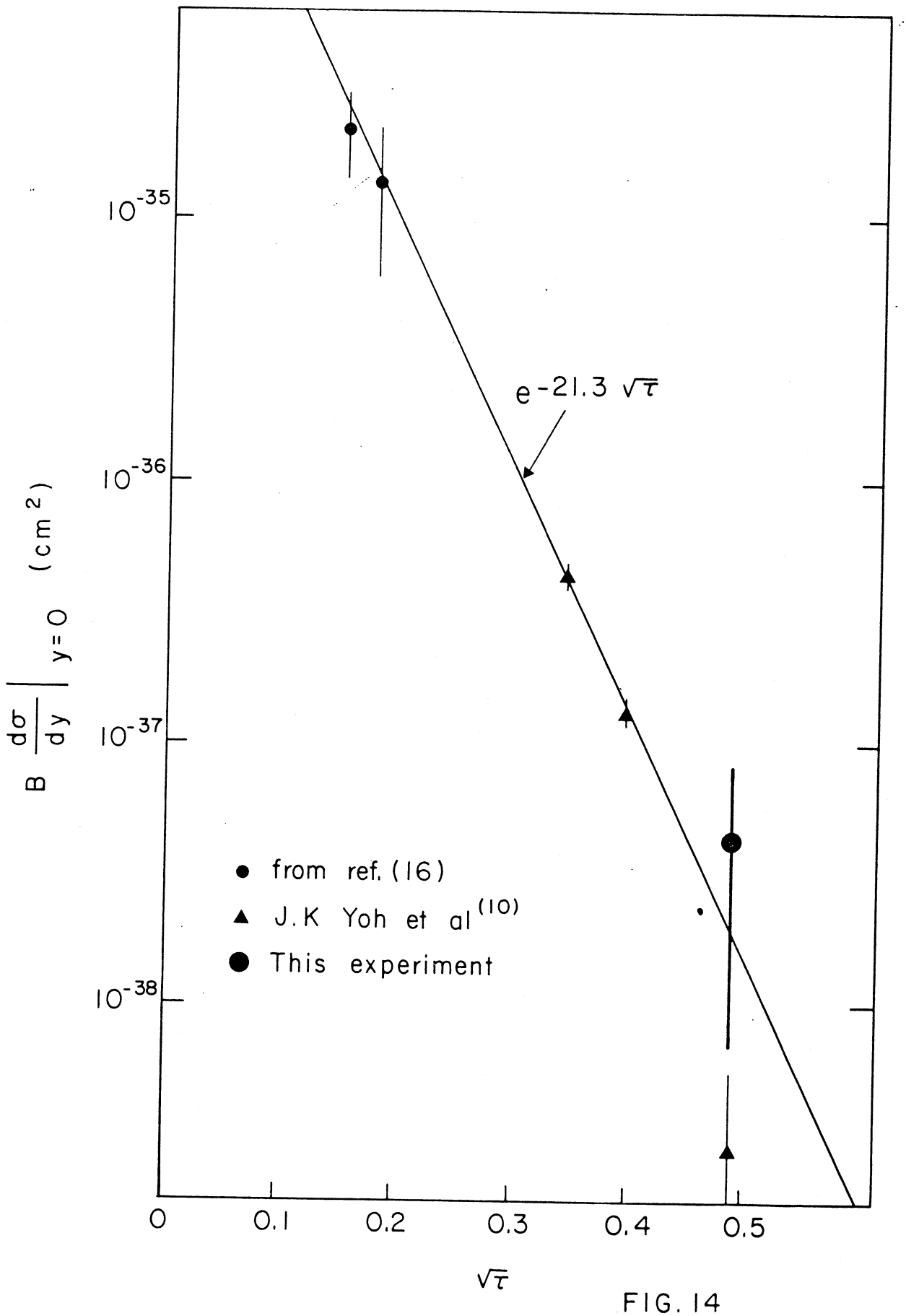
$B \left.\frac{d\sigma}{dy}\right|_{y=0}$ (cm^2)
10^{-35}
10^{-36}
10^{-37}
10^{-38}
$e^{-21.3\sqrt{\tau}}$
● from ref. (16)
▲ J.K Yoh et al (10)
● This experiment
0
0.1
0.2
0.3
0.4
0.5
$\sqrt{\tau}$

FIG. 14